Proc. VIIth Digital Image Computing: Techniques and Applications, Sun C., Talbot H., Ourselin S. and Adriaansen T. (Eds.), 10-12 Dec. 2003, Sydney

3D Face Recognition using Longitudinal Section and Transection

Yeunghak Lee
214-1 Dae-dong Kyongsan-si Kyongbook
SEECS Yeunganam Univ. 712-749, Korea
annaturu@yumail.ac.kr

Abstract. In this paper, a new practical implementation of a person verification system using features of longitudinal section and transection and other facial, rotation compensated 3D face image, is proposed. The approach works by finding the nose tip that has a protrusion shape on the face. In feature recognition of 3D face image, one has to take into consideration the orientated frontal posture to normalize. Next, the special points in regions, such as nose, eyes and mouth are detected. The depth of nose, the area of nose and the volume of nose based both on a longitudinal section and transection are calculated. The eye interval and mouth width are also computed. Finally, the 12 features on the face were extracted. The L1 measure for comparing two feature vectors were used, because it is simple and robust. In the experimental results, proposed method can be made recognition rate of 95.5% for the longitudinal section and transection.

1 Introduction

Biometric authentication technologies such as face, finger, hand, iris, and speaker recognition are available today and already in use. In biometric identification system, because face recognition is non-touch style, it is challenging area of research, next to fingerprinting. For visible spectrum imaging, there have been many studies reported in literature for last 30 years [1]. But the method has been found to be limited in their application. It is influenced by lighting illuminance and encounters difficulties when the face is angled away from camera. These factors cause low recognition. To solve these problems a computer company has developed a 3D face acquisition systems [2, 3]. Broadly speaking the two way to establish recognition employs the face feature based approach and the area based approach [4, 5].

Feature based approach is that a face can be recognized even when the details of the individual features (such as eyes, nose and mouth) are no longer resolved. This is to extract relative position and other parameters of distinctive features such as eyes, mouth, nose and chin. And template based approach is that, in the simplest version of template matching, visual patterns, represented as bidimensional array of intensity values, are compared using suitable metric. But it needs too much memory to process, the speed also slow to calculate and the database construction is difficult.

In this paper, we introduce a novel face recognition using the geometrical features of normalized 3D face images. The first approach works by finding nose tip that has a protrusion shape on the face, nose bridge, nose base, mouth, and etc. Following works are to extract important scalar features for the purpose of discriminating individual faces using previously mentioned points. The rest of the paper is structured as follows. In section 2, the normalization for the oriented faces is presented. In section 3, the overview of feature extraction is explained. Experimental results for 3D images are shown in section 4, and conclusions are given in section 5.

2 Face normalization

The nose tip (fiducail point) is easy to find using average threshold method, because it has a protrusion shape on the face [6]. From this fiducial point, the oriented faces are compensated for three axes, X, Y, and Z.

In feature recognition of 3D faces, one has to take into consideration the obtained frontal posture. Face recognition systems suffer drastic losses in performance when the face is not correctly oriented. The normalization process proposed here is a sequential procedure that aims to put the face shapes in a standard spatial position. The processing sequence is panning, rotation and tilting. Firstly, for the panning, the face is panned by angle which is defined by the mean and distance of the depth value of local areas that are divided into right and left, as defined in (1), (2), (3) and (4). The window size used is 30x30, with the nose tip as the reference point. For example, the given binary images presented in Fig. 1 are before compensation (BC) and after compensation (AC) for panning.

$$X_L = \frac{1}{n}\sum_{i=s1}^{s1-30} x_i \quad \text{and} \quad X_R = \frac{1}{n}\sum_{i=s2}^{s2+30} x_i \tag{1}$$

$$M_L = \frac{1}{n}\sum_{i=s1}^{s1-30}\sum_{j=\max\_y}^{\max\_y-30} D_{img}, \quad \text{if } D_{img} > 0 \quad M_R = \frac{1}{n}\sum_{i=s2}^{s2-30}\sum_{j=\max\_y}^{\max\_y+30} D_{img}, \quad \text{if } D_{img} > 0 \tag{2}$$

$$L = X_L - X_R \quad \text{and} \quad M = M_L - M_R \tag{3}$$

$$\theta = \tan^{-1}\left(\frac{M}{L}\right) \tag{4}$$

X_L: centroid of left area $\qquad$ X_R: centroid of right area

M_L: mean value of left local area $\qquad$ M_R: mean value of right local area

L: difference of two centroid value $\qquad$ M: difference of two mean value

θ: rotated angle $\qquad$ s1: max_x-15

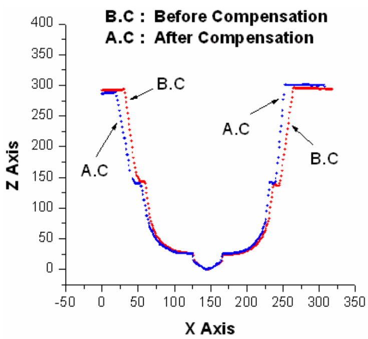

Fig. 1 The processing of panning. BC is before compensation and AC is after compensation.

Secondly, for the rotation, the face is rotated by angle which is defined by the modified centroid and moments used in several area [16]. In general, centroid and moments are given as the equivalent of their continuous counterparts. Given *B*, which is the binary image, a set of *n* pixels $p_i = (x_i, y_i)$ (i=1,…,*n*), the coordinates (x_q, y_q) of the centroid q of *B* are calculated by

$$x_q^p = \frac{1}{n}\sum_{i=11}^{n} x_i^p \quad \text{and} \quad y_q^p = \frac{1}{n}\sum_{i=11}^{n} y_i^p \tag{5}$$

where *p* is contour line threshold values, p=15,16,17,18,19,20.

Moments allow for a unique characterization of a shape. Given *B*, a set of *n* pixels $p_i = (x_i, y_i)$ (i=1,…,n), and $q = (x_q, y_q)$ its centroid, the definition of the discrete (*k*, *l*)-order central moment $\Pi_{k,l}^p$ of the set B is given by

$$\Pi_{k,l}^p = \sum_{i=1}^{n} (x_i^p - x_q^p)^k (y_i^p - y_q^p)^l \tag{6}$$

A shape is uniquely represented by the set of all its (k, l)-ordered central moments (k, l∟**N**). Clearly, the shape of the face is symmetrical with respect to the diagonal axis or nose bridge, $\Pi_{k,l}^p = \Pi_{l,k}^p$ for all *k*∟ **N** and *l* ∟ **N**. Orientation is defined as an angle θ representing the angle made between the axis and the axis of least moment of inertia. The value of angle is obtained by the following formula (7).

$$\theta = \frac{1}{6}\sum_{p=15}^{20}\left(\frac{1}{2}\tan^{-1}\left(\frac{2\Pi_{1,1}^{p}}{\Pi_{2,0}^{p} - \Pi_{0,2}^{p}}\right)\right) \tag{7}$$

In Fig. 2, original image, rotated image and the binary images by the contour lines threshold value are presented.

Third, for tilting, after finding the nose bridge and the nose base, the face is adjusted until the difference depth value of two points is became 10, as shown in Fig. 3. In this figure, the red profile line (B.C.) is before tilting and the blue profile line (A.C.) is after tilting.

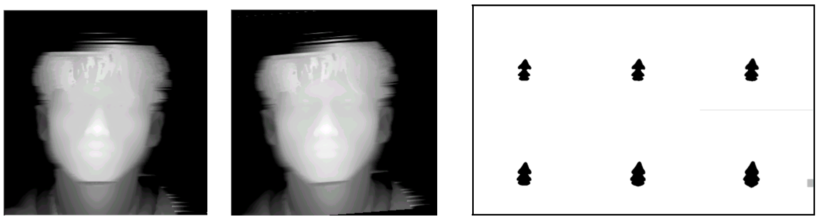

(a) (b) (c)

Fig. 2 The processing of rotation (a) before rotation (b) after rotation (c) binary image by contour line threshold value p=15,16,17,18,19,20 from image.

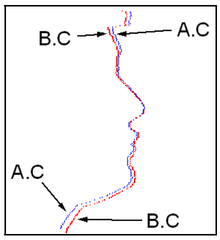

Fig. 3 The processing of tilting. BC is before tilting and AC is after tilting.

3 Feature extraction and scalar features from 3D images

The scalar features are extracted from concaves consisted on curves, except nose tip. And we can easily find that the smallest value is feature point. So concaves are found that the nose base and the nose bridge are used 5x1 window, and the end of nose left and the end of nose right are used 1x5 window. Fig. 4 (a) shows each feature points, and Fig. 4 (b) shows the result of the extraction of features. In this thesis, we adapted 12 features values. It includes that the side view area and the depth value, which the reference is longitudinal section, the frontal view area and the depth value, which the reference is transection, and the volume of nose. And we define that, the a is the nose point, the b is the nose bridge, the c is the nose base, the d is the end of left nose and the e is the end of right nose.

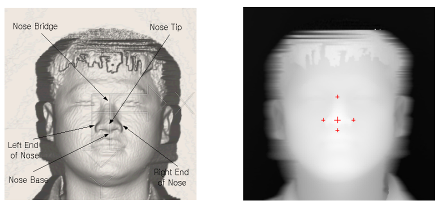

(a) (b)

Fig. 4 The feature points and the result of the feature points extraction (a) the definition of feature points (b) the result of feature points.

3.1 The depth, area and angle of longitudinal section

The depth (f1) of normal line is from point a to strait line b-c, which is perpendicular to normal line, as shown Fig. 5 (a). Equation (8) and equation (9) present relation between a point and strait line, the f1 is calculated by

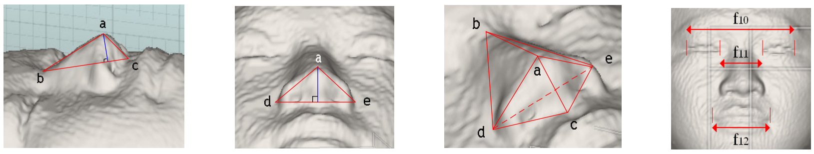

(a) (b) (c) (d)

Fig. 5 3 dimensional expression of feature points for longitudinal section and transection and other scalar features (a) the depth of longitudinal section (b) the depth of transection (c) the volume of nose (d) other scalar features.

$$kz + ly + m = 0$$
$$(y_2 - y_1)z_0 + (z_1 - z_2)y_0 + \{y_1(z_2 - z_1) - z_1(y_2 - y_1)\} = 0 \tag{8}$$

$$f_1 = \frac{|k * z_0 + l * y_0 + m|}{\sqrt{k^2 + l^2}} \tag{9}$$

where k, l, and m are constant..

Therefore the equation of the area of triangle is “base*height/2”, if strait line b-c is D_3, the area of longitudinal section (f2) calculated by

$$f_2 = \frac{1}{2} * D_3 * f_1 = \frac{1}{2} * \left| k * z_0 + l * y_0 + m \right|$$

$$= \frac{1}{2}\left| (y_2 - y_1)z_0 + (z_1 - z_2)y_0 + \{y_1(z_2 - z_1) - z_1(y_2 - y_1)\} \right| \tag{10}$$

The angle of longitudinal section (f3), $\angle bac$, is calculated by

$$f_3 = \sin^{-1}\left(\frac{2 * f_2}{t_1 * t_2}\right) \tag{11}$$

where t_1 is strait line a-b and t_2 is strait line a-c.

3.2 The depth, area and angle of transection

The depth of normal line is from point a to strait line d-e, which is perpendicular to normal line, as shown Fig. 5 (b). The depth of teansection(f4) is calculated by

$$f_4 = \frac{|k * x_0 + l * z_0 + m|}{\sqrt{k^2 + l^2}} \tag{12}$$

where k, l, and m are constant..

If strait line b-c is D_4, the area (f5) of transection calculated by

$$f_5 = \frac{1}{2} * D_4 * f_3 = \frac{1}{2} * \left| k * x_0 + l * z_0 + m \right|$$

$$= \frac{1}{2} \left| (z_4 - z_3) x_0 + (x_3 - x_4) z_0 + \{ z_3 (x_4 - x_3) - x_3 (z_3 - z_3) \} \right| \quad (13)$$

And the angle (f6) of longitudinal section, $\angle dae$, is calculated by

$$f_6 = \sin^{-1}\left(\frac{2 * f_5}{t_1 * t_2} \right) \quad (14)$$

where t_1 is strait line a-d and t_2 is strait line a-e.

3.3 The volume of nose

As shown in Fig. 5 (c), the volume of nose is composed of the tetrahedral abde and acde. For the volume of each tetrahedral v1 and v2, firstly, the distance of between point b and point c and plane which includes Δ ade is calculated. The volume of tetrahedral (v1) using the equation (9) and (10) which is plane equation is calculated. The plane equation which includes three points, a(x_0,y_0,z_0), d(x_4,y_0,z_3) and e(x_4,y_0,z_4) is given by

$$kx + ly + mz + n = 0 \quad (15)$$

$$\begin{vmatrix} x & y & z & 1 \\ x_0 & y_0 & z_0 & 1 \\ x_3 & y_0 & z_3 & 1 \\ x_4 & y_0 & z_4 & 1 \end{vmatrix} = 0 \quad (16)$$

where k, l, m and are constant [7].

Using equation (16), D5, the distance from the point b(x_0,y_1,z_1) to plane, and D6, the distance from the point c(x_0,y_2,z_2) to plane are calculated by

$$D_5 = \frac{| k * x_0 + l * y_1 + m * z_1 + n |}{\sqrt{k^2 + l^2 + m^2}} \quad (17)$$

$$D_6 = \frac{| k * x_0 + l * y_2 + m * z_2 + n |}{\sqrt{k^2 + l^2 + m^2}} \quad (18)$$

Finally, the volume (f7) of nose is given by

$$f_7 = v_1 + v_2 = \frac{1}{3} * D_5 * f_5 + \frac{1}{3} * D_6 * f_5$$

$$= \frac{1}{3} * f_5 * (D_5 + D_6) \quad (19)$$

3.4 The other scalar features

As shown in Fig. 5 (c), the angle (f8) of nose bridge, $\angle dce$, and the angle (f9) of nose base, $\angle dce$, are calculated by equation (12). Additionally the distance of the eye cavity (outside corner), f10, the distance of the eye cavity (inside corner), f11, and the length of mouth, f12 are calculated. For these parameters, in this paper used maximum curvature which is presented the curvature of face surface, the result are shown in Fig. 6, in here, $K_{\max}$ is over 0.5. The process of erosion and dilation was conducted to extract the shape of mouth and eye area.

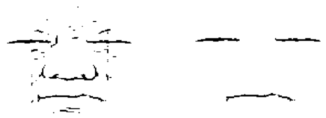

(a) (b)

Fig. 6 The extraction of mouth and eyes using the maximum curvature and dilation and erosion (a) the result of using maximum curvature (b) the result of morphology processing.

4 Experimental results

In this study, we used a 3D laser scanner made by a 4D Culture to obtain a 3D face image. First, a laser line beam was used to strip the face for 3 seconds, thereby obtaining a laser profile image that is, 180 pieces. The obtained image size is extracted by using the extraction algorithm of line of center, which is 640x480. Next, calibration is done in order to process the height value, resampling and interpolation. Finally, a 3D face image using this paper is extracted, at 320x320. The database is used to compare the different strategies and is composed of 50 images (two images of 25 people). Of the two pictures available, the second photos were taken at a time interval of 30 minutes.

This paper tried two kinds of experimental: the first is the verification of normalization for the oriented images and the second is the comparative of similarity between query image and database images from extracted features. The similarity of the indexing system used L1-norm to compare query with database for features.

4.1 The Experiment of the compensation of orientation

Table 1 represents the result of recognition rate for features, f1, f2, f4, f5, and f7. The depth (f4) and the area (f5) of longitudinal section is represented higher recognition rate and the area (f2) of transection is represented the lowest recognition rate. To improve the recognition rate, we adapted the weighted value for each features, because each features have lower identification. The result w1 and w2 represent more improved recognition rate in Table 1. The w1 results that each features were applied same weighted value, and the w2 results that each features were applied different weighted values according to the each recognition rate. And the RT is “ranked threshold”, in table 1.

$$diff = \sum_{i=1}^{5} \left| (w_i * f_i)_{Original\_img} - (w_i * f_i)_{DB\_img} \right| \tag{20}$$

Table 1. The comparison of each features recognition rate

RT	5	10	15
F1	54%	74%	84%
F2	30%	64%	86%
F4	66%	90%	96%
F5	64%	96%	100%
F7	46%	82%	100%
W1	86%	100%	100%
W2	94%	100%	100%

To establish the compensation of orientation for suggested method in this paper, we executed three kinds of test: before the compensation, the change of compensation order for the y-axis and the z-axis. As the expected, the compensated images are better than not compensated images and the y-axis is better than the x-axis, in the compensation order for the oriented images, as shown in Table 2.

Table 2. The comparison of before and after compensation

RT	Before Compensation	After compensation	
		$\theta_Z - \theta_Y - \theta_X$	$\theta_Y - \theta_Z - \theta_X$
5	78.0%	90.0%	94.0%
10	96.0%	96.0%	100%
15	98.0%	98.0%	100%

4.2 The recognition rate

For the second experiment, the database added 6 images included a little noise, except the used images in 4.1. Fig. 7 shows the result of recognition for feature vectors. The depth (f4) of longitudinal section was the primary recognition rate when rank threshold is 5, and if ranked threshold is 10, the area (f5) of longitudinal section was the best recognition rate, 82.14%. Table 3 shows the recognition ranking for feature vectors.

Table 3. The recognition ranking of feature vectors

Recognition rank	Ranked Threshold			Recognition rank	Ranked Threshold		
	5	10	15		5	10	15
1	F4	F5	F4	7	F3	F3	F2
2	F5	F4	F5	8	F6	F2	F8
3	F7	F7	F7	9	F2	F6	F6
4	F8	F11	F1	10	F12	F12	F9
5	F11	F8	F3	11	F9	F9	F12
6	F1	F1	F11	12	F10	F10	F10

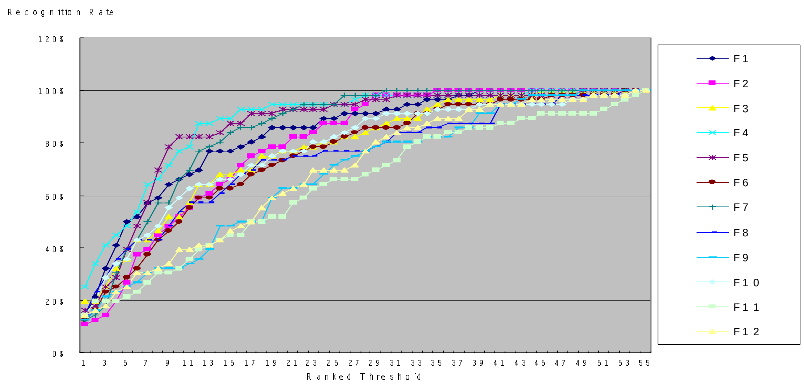

Fig. 7 The results and compare of scalar Features

Fig. 8 shows the recognition rate that features vectors are accumulated from ranking 1 to ranking 12 according to the recognition rate. For example, X value is 3, and if rank threshold is 5, accumulation order is f4, f5, and f7. So the recognition rate for three feature vectors added the weighted value, which has the same value, is 71.43%.

As shown in Fig. 8, the recognition rate is declined because of including the feature vectors of lower rank: f9, f10, f11 and f12, and other feature vectors promote for the recognition rate. This is because of miss finding for each measurement points, that is because of the crow's-feet of the eye or mouth and a dimple

5. Conclusion

In this paper, a new practical implementation of a person verification system using features of longitudinal section and transection and other facial, rotation compensated 3D face image, is proposed. In feature recognition of 3D face image, one took into consideration the orientated frontal posture to normalize using the nose information and longitudinal section and transection information. From normalized image, the special points in regions, such as nose, eyes and mouth are detected. The depth of nose, the area of nose and the volume of nose based for both on the longitudinal section and transection are calculated. The eye interval and mouth width are also computed. The recognition rates for feature vectors were accumulated weighted value from ranking 1 to ranking 12 according to the recognition rate, and when the rank threshold was 5, the recognition rate was 95.5%. From the experimental results, we confirmed that the compensation of orientation was more improved to 12~16%, in case Y-axis was conducted preferentially., among the feature vectors on the face. And we prove that the geometrical features of nose area have superior recognition rate than using feature vectors of eye and mouth. We consider that there are many future experiments that could be don to extend this study.

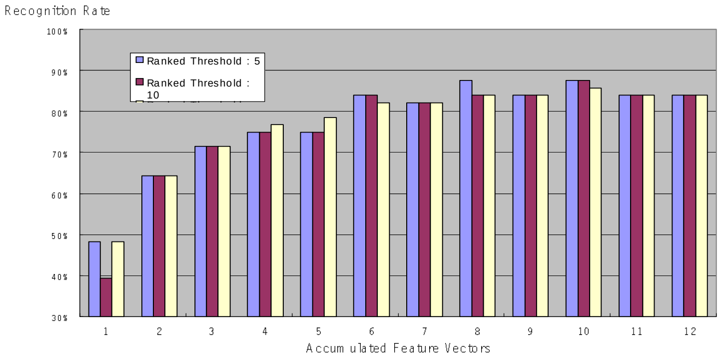

Fig. 8 The compare of the accumulation of rank according the recognition rate of feature vectors

References

1. R. Chellappa, C. L. Wilson and S. Sirohey "Human and Machine recognition of faces: A Survey", *Preceeding of the IEEE*, Vol.83, No.5, 705-740, 1995.
2. 4D Culture, "http://www.4dculture.com".
3. Cyberware, "http://www.cyberware.com".
4. P. L. Hallinan, G. G. Gordon, A. L. Yuille, P. Giblin and D. Mumford *Two- and three-dimensional patterns of the face*, A. K. Peters, Ltd., 1999.
5. R. Brunelli and T. Poggio, "Face Recognition: Features versus Templates", *IEEE Trans. PAMI*, Vol. 15, pp. 1042-1052, 1993.
6. Y. H. Lee, K. W. Park, J. C. Shim and T. H. Yi, "3D Face Recognition using Projection Vectors", *Preceeding of IVCNZ2002*, pp. 151-156, 2002.
7. Mathematics Book Publishing Committee, *Linear algebra and Geometry*, Hyungseul Publishing Co., 1992.